Poly(ether ether ketone) Composites Reinforced by Short Carbon Fibers and Zirconium Dioxide Nanoparticles: Mechanical Properties and Sliding Wear Behavior with Water Lubrication

Y. J. Zhong, G. Y. Xie, G. X. Sui, R. Yang

Institute of Metal Research, Chinese Academy of Sciences, Shenyang, China 110016

ABSTRACT: Poly(ether ether ketone) (PEEK) composites reinforced by short carbon fibers (SCFs) and nanoscale zirconium dioxide (ZrO_2) particles were prepared by twin-screw extrusion compounding and subsequently injection molding. The effects of SCFs and ZrO_2 nanoparticles on the mechanical properties and wear behavior of PEEK composites with water lubrication were investigated. The mechanical properties of the composites were dramatically enhanced by the incorporation of SCFs. The addition of nano-ZrO_2 also promoted efficient improvements in the stiffness and hardness but degraded the impact strength. The compounding of the two fillers remarkably improved the wear resistance of the composites under aqueous conditions and especially under high pressures. The excellent wear resistance of the PEEK/carbon fiber (CF)/ZrO_2 composites under aqueous conditions was revealed to be due to a synergy effect between the ZrO_2 nanoparticles and CFs. The SCFs carried the majority of the load during a sliding process and prevented severe wear of the matrix. The incorporation of nano-ZrO_2 efficiently inhibited CF failure by reducing the stress concentration on the CF interface and the shear stress between two sliding surfaces via a positive rolling effect of the nanoparticles. Furthermore, a linear correlation was found between the wear rate and some mechanical properties of the composites. © 2010 Wiley Periodicals, Inc. J Appl Polym Sci 119: 1711–1720, 2011

Key words: composites; high performance polymers; mechanical properties; morphology

INTRODUCTION

Because many industrial devices and components made of steel or alloys that involve relative motion in aqueous environments are prone to corrosion, it is valuable in science and is significant in engineering to develop polymer–matrix composites as potential substitutes for metallic materials for the sake of improved corrosion resistance in aqueous media and light weights. The properties required for a tribological matrix include a high service temperature, good chemical resistance, high mechanical properties, high wear resistance, and outstanding cohesive strength. Within this framework, poly(ether ether ketone) (PEEK) is regarded as one of the most promising polymer materials for tribological applications in aqueous environments. The tribological performance of neat PEEK under aqueous conditions was reported by Yamamoto and Takashima.[1] However, it seems that neat PEEK exhibits relatively poor wear resistance with water lubrication in some cases. To facilitate more applications by enhancing the anti-wear properties of PEEK, various types of fillers have been incorporated into PEEK under different conditions.

Excellent candidates for many tribological applications, short carbon fibers (SCFs) are widely used in PEEK composites for which wear resistance is an important issue, even at elevated temperatures and under aqueous conditions.[2–10] Generally, SCFs can increase the creep resistance, hardness, and compressive strength of PEEK composites and reduce their adhesion to their counterpart and the frictional heat in the contact area. Furthermore, the fibers carry the main load between the contacting surfaces,[11] so carbon fiber (CF) reinforced PEEK always shows excellent wear resistance with water lubrication.[2,10] Hence, the mechanical and tribological performances of PEEK composites can be greatly improved by the incorporation of SCFs.

Nanoparticle-reinforced polymers are attracting more and more attention because of their unique properties resulting from the nanoscale structures. The extremely high specific surface area facilitates the creation of a great amount of interphase in composites and a strong interaction between the fillers and the matrix. Some nanometric inorganic fillers

TABLE I
Mechanical Properties of PEEK and PEEK/10CF/ZrO$_2$ Composites

No.	PEEK/CF/ ZrO$_2$ (wt %)	Tensile strength (MPa)	Young's modulus (GPa)	Fracture strain (%)	Impact strength (kJ/m^2)	Microhardness (kg/mm^2)
0	100/0/0	98.1 ± 1.3	3.70 ± 0.04	21.62 ± 0.87	6.73 ± 1.31	21.9 ± 1.0
A1	90/10/0	145.0 ± 2.2	9.40 ± 0.29	2.90 ± 0.11	9.11 ± 0.77	25.3 ± 0.9
A2	85/10/5	156.9 ± 2.2	9.73 ± 0.10	3.54 ± 0.12	8.86 ± 0.29	25.5 ± 2.4
A3	80/10/10	161.1 ± 1.3	10.41 ± 0.34	3.06 ± 0.12	8.13 ± 0.58	26.8 ± 2.4
A4	75/10/15	167.9 ± 1.5	11.55 ± 0.22	2.63 ± 0.27	7.37 ± 0.19	28.4 ± 2.1
A5	70/10/20	171.2 ± 1.7	12.31 ± 0.09	2.42 ± 0.24	6.63 ± 0.32	30.6 ± 1.5

have been demonstrated to have the ability to reduce the friction and wear of polymers. In the case of PEEK matrix nanocomposites, small amounts of inorganic nanoparticles, such as silicon nitride, silicon dioxide, silicon carbide, and zirconium dioxide (ZrO$_2$), contribute to reductions in the friction coefficient and wear rate under dry-sliding conditions.[12–17] Wang et al.[18,19] investigated the effects of nanometric particles on the tribological behaviors of PEEK with water lubrication and found that the enhancement of the wear resistance should be attributed to the improvement in the formation of a high-quality transfer film by the incorporation of silicon carbide nanoparticles. However, an efficient transfer film could not be formed easily in some other cases. Moreover, the wear behaviors of the composites are also affected by the proportion of the nanoparticles. The wear rates of the nanocomposites always achieve a minimal value with increasing filler content. With excessive nanofiller content, particle agglomeration might degrade the wear performance.[14] A homogeneous dispersion of the nanoparticles and good particle–matrix bonding have been thought to have further benefit for property improvements.[20,21]

Recently, some investigations of the effects of hybrid reinforcement by inorganic submicro/nanoparticles and SCFs on the tribological behavior of polymers composites under dry-sliding conditions have been conducted.[22–26] It is believed that there is a synergistic effect of SCFs with fine particles on the enhancement of the wear resistance. The protection of the SCF–matrix interface by the nanoparticles and a rolling effect of the nanoparticles between the material pairs have been proposed. However, there is no report on the tribological behavior and wear mechanism of inorganic submicro/nanoparticles compounding with CF hybrid composites with water lubrication. In this work, the mechanical performances and tribological behaviors of PEEK composites reinforced with CFs and nano-ZrO$_2$ particles with water lubrication were investigated. The effects of CFs and ZrO$_2$ nanoparticles on the wear performance were studied. Furthermore, the relationships between the mechanical properties and wear behaviors were also examined.

EXPERIMENTAL

Materials

Commercially available PEEK and PEEK with 30% CF were supplied by Degussa Co., Ltd., Germany. ZrO$_2$ nanoparticles with an average size of 80 nm were supplied by Nanjing Haitai Nano Co., Ltd., China.

Specimen preparation

The PEEK/CF/ZrO$_2$ composites were divided into two groups: PEEK/10CF/ZrO$_2$ (group A) and PEEK/CF/10ZrO$_2$ (group B). The compositions of the two PEEK composite groups are listed in Tables I and II. For comparison, neat PEEK and PEEK composites filled individually with 10 wt % CF (PEEK/10CF) or 10 wt % ZrO$_2$ (PEEK/10ZrO$_2$) were also prepared. The PEEK grade with 30% CF was used as the master batch to dilute the aforementioned compositions. The compounding of different grades of PEEK with the nanoparticle fillers was achieved with a twin-screw extruder at a screw speed of 360 rpm and a processing temperature of 390°C. All the materials were dried in an oven at 150°C for 6 h

TABLE II
Mechanical Properties of PEEK/CF/10ZrO$_2$ Composites

No.	PEEK/CF/ ZrO$_2$ (wt %)	Tensile strength (MPa)	Young's modulus (GPa)	Fracture strain (%)	Impact strength (kJ/m^2)	Microhardness (kg/mm^2)
B1	90/0/10	102.8 ± 0.1	3.91 ± 0.05	19.05 ± 1.87	6.30 ± 0.32	22.7 ± 0.8
B2	80/10/10	161.1 ± 1.3	10.41 ± 0.34	3.06 ± 0.12	8.13 ± 0.58	26.8 ± 2.4
B3	75/15/10	191.4 ± 1.3	13.54 ± 0.15	2.29 ± 0.05	8.57 ± 0.26	29.3 ± 1.8
B4	70/20/10	215.5 ± 1.2	17.62 ± 0.45	2.08 ± 0.01	9.36 ± 0.64	34.2 ± 4.0

before melt processing. The extrudate was continuously cooled by water and pelletized. The pellets were dried in an oven at 150°C for 6 h before injection molding. Standard test bars were injection-molded at a mold temperature of 180°C.

Wear tests

Wear tests were conducted on an MM-W1A universal wear-testing machine (Jinan Shijin Co., Ltd., China) using a three-pin-on-disk configuration. Both the cylindrical specimen pins (4.8 mm in diameter and 12.8 mm long) and the stainless steel counterpart disk (4Cr13, HV476) were polished with 1500-grit silicon carbide water-abrasive paper. The average roughness of the counterface was 0.038 μm. All the tests were carried out at the ambient temperature over a period of 2 h at a sliding velocity of 2.0 m/s. The applied load ranged from 1 to 8 MPa. The polymer–metal interface was immersed in tap water. Before and after the test, the pins were ultrasonically cleaned and dried at 150°C for 3 h before weighing. Then, the mass loss of the composite pins was measured with a Mettler AE240 (Switzerland) electronic balance (accuracy = 0.01 mg) for the calculation of the specific wear rate. The specific wear rate (K) was calculated after the test with the following equation:

$$K = \frac{\Delta m}{\rho F_N L} \quad (1)$$

where Δm is the mass loss of the pins (mg), ρ is the density of the pins (g/cm^3), F_N is the applied load (N), and L is the total sliding distance (m). Three replicated friction and wear tests were performed for each specimen to minimize data scattering, and the average of the three replicate test results is reported as the specific wear rate in this work.

Mechanical properties

Tensile tests were carried out on a universal testing machine (Zhineng Instrument Co. Ltd., Changchun, China) with a crosshead speed of 5.0 mm/min. A load cell of 20 kN and an extensometer with a gauge length of 25 mm were used. The parallel segment of the dumbbell-shaped specimens for tensile tests was 30 × 5 × 4 mm^3. Notched Charpy impact tests were carried out on a JJ-5 pendulum impact apparatus (Zhineng Instrument Co. Ltd., Changchun, China) according to ASTM D 6110. For each specimen, the data reported here represent the average results of at least five successful tests. The microhardness was measured with a Future-Tech (Japan) FM-700e Vickers microhardness tester. A load of 100 gf with a loading time of 10 s was applied. At least 10 data points were collected to calculate the microhardness value for each specimen.

Morphological observation

After the test, the worn surfaces of the composite and the counterface and also the wear debris were coated with a thin layer of gold and then examined with a JSM-6301F (Japan) scanning electron microscope.

RESULTS AND DISCUSSION

Mechanical properties

Tables I and II show the results of tensile, notched impact, and microhardness tests for the two groups of PEEK composites as well as neat PEEK. The tensile strength, Young's modulus, and microhardness were evidently enhanced by the addition of the two fillers. The composite filled with 10% ZrO_2 nanoparticles showed slight increases in the tensile strength and Young's modulus versus neat PEEK. Meanwhile, the incorporation of 10% CF into neat PEEK led to increases of 48% and 1.5 times in the tensile strength and Young's modulus, respectively. An ascending trend with the filler loading for the tensile strength, Young's modulus, and microhardness was found for the hybrid composites. The tensile strength linearly increased from 145 MPa for composite A1 to 171 MPa for composite A5 with a growth rate of 17.9% as the content of ZrO_2 nanoparticles increased from 0 to 20 wt %. Simultaneously, Young's modulus and the microhardness increased by 31.0 and 20.9%, respectively. As for group B, as the CF content changed from 0 to 20 wt %, the highest values of the tensile strength, Young's modulus, and microhardness were 2.1, 4.5, and 1.5 times the lowest values, respectively. Although both fillers had obvious reinforcement effects for neat PEEK, the more significant enhancements of group B showed that the SCFs played a key role in improving the mechanical performances of PEEK.

In contrast, the elongation at break of the hybrid composites dropped sharply with the incorporation of both fillers and decreased gradually with increasing filler content because the fillers restricted the motion of polymer chains physically or chemically.[27] The fracture strain of PEEK/10ZrO$_2$ was only a little lower than that of neat PEEK. However, a rapid drop was found for the PEEK/10CF composites. Therefore, the addition of fillers, especially with the compounding of CFs, degraded the tensile ductility in this case.

Apparently, the two fillers had opposite influences on the notched Charpy impact strength. The incorporation of CFs into PEEK resulted in the enhancement of the impact strength, and the impact strength significantly increased with increasing CF content. However, the filled nano-ZrO$_2$ reduced the impact strength of the composites. As is known, the impact

energy is consumed primarily during crack initiation and secondarily during crack propagation. On the one hand, when fillers are incorporated into polymers, they enhance the composites and restrict crack initiation; on the other hand, the fillers might restrain the molecular motion and thus reduce the amount of energy consumed in matrix plastic deformation. The different effects of the two fillers on the impact strength could be attributed to the differences in their shapes and sizes (especially the reinforcement mechanism). The CFs possessed a reinforcement efficiency superior to that of the nano-ZrO_2 particles. In addition, the energy spent in pulling the CFs from the PEEK matrix played an important role during crack propagation. Therefore, the CFs resulted in higher fracture resistance to the fracture failure of the composites.

Tribological properties

The results for the friction coefficient and wear rate of two typical PEEK/CF/ZrO_2 hybrid composites chosen from the two composite groups against stainless steel as a function of the applied load with water lubrication are presented in Figure 1. Figure 1(a) shows that although the friction coefficients of the PEEK/10CF/20ZrO_2 and PEEK/20CF/10ZrO_2 composites fluctuated with different loads, they were all at a level of approximately 0.01. Meanwhile, both composites exhibited dramatic wear performances at different loads. As shown in Figure 1(b), the wear rates of the hybrid composites all showed a reduction with the applied load increasing. The lowest wear rates were achieved at 8 MPa for both composites, and they were almost 1 order of magnitude lower than those at 1 MPa.

Commonly, an applied load affects wear behavior in many ways. Sliding between materials results in heat generation and hence increases the temperature of two frictional surfaces. A high applied load always leads to a temperature increase at the rubbing surfaces under dry-sliding conditions. Thus, the polymer surface might be plasticized, and this might be followed by a decrease in the carrying capacity, which facilitates the easy detachment of the polymer and results in severe wear. However, for the CF-reinforced composites, the wear rate was almost not affected by the load until a critical value was reacehd.[6] Besides, water could act as a cooling agent in this case, and this meant that friction-induced thermal and mechanical effects might be inhibited in an aqueous environment. Actually, the temperature increases of the water under various loads were all less than 10°C under the conditions used for all the hybrid composites, and this showed that the heat could be efficiently dissipated from the sliding surface. Apparently, PEEK/CF/ZrO_2 hybrid composites
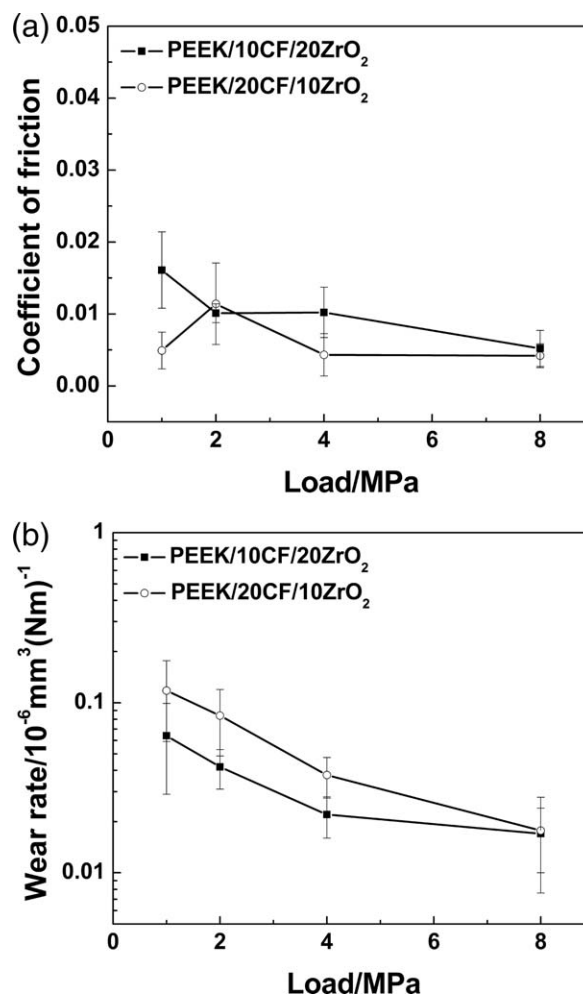

Figure 1 Effect of the load on (a) the friction coefficient and (b) the wear rate of the PEEK/10CF/20ZrO_2 and PEEK/20CF/10ZrO_2 composites (test conditions: water lubrication, 2 m/s sliding velocity, and 2-h sliding duration).

are suitable for wear applications with water lubrication, especially under high loads.

Effect of CFs

Generally, CFs can effectively improve the wear resistance of polymer composites by serving as fundamental load-bearing elements during the wear process under dry conditions.[11] However, this might be different under aqueous conditions because water can act as a cooling agent and lubricant medium. Water also takes away the wear debris between the sliding surfaces, and this will influence the formation of a transfer film.[28,29] Therefore, the wear mechanism of CFs needs to be clarified in this case. Figure 2 shows the friction coefficients and wear rates of PEEK/CF/10ZrO_2 composites with various amounts of CFs under different applied loads and aqueous conditions. Under 1 MPa, the friction coefficients fluctuated around 0.01, and the wear rate
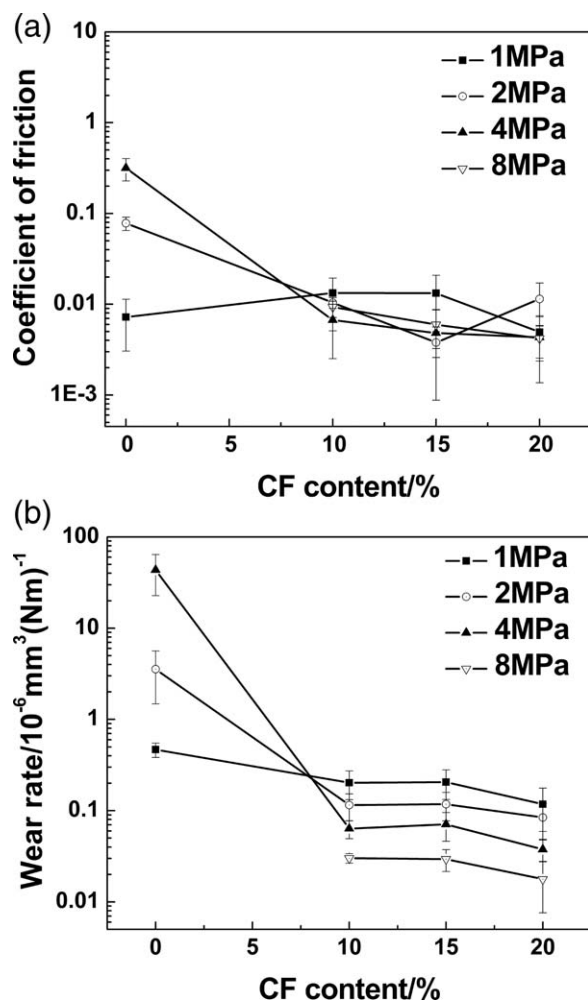
around 0.01. The wear rates of the hybrid composites varied with the CF content and the applied load. With the CF content between 10 and 15 wt %, the wear rates were almost at the same level. After that, the wear rates decreased and finally reached the lowest value when the CF content reached 20 wt %. The lowest wear rate of 1.77×10^{-8} mm^3/Nm was achieved when the load was 8 MPa for the PEEK/20CF/10ZrO$_2$ composite. It can be concluded that PEEK composites with CFs exhibit better wear resistance under high pressures in water.

To identify the wear mechanism of the PEEK composites and the effects of the CFs and load on the wear rate, the morphologies of the worn surfaces for the PEEK/10CF/10ZrO$_2$ composite at 1 and 4 MPa were observed with scanning electron microscopy (SEM), as shown in Figure 3. The worn surfaces under both conditions were characterized by mild ploughing and microsurface damage caused by mild fatigue wear. This indicated that the main wear mechanism of the hybrid PEEK composites consisted of mild abrasion and fatigue wear. Figure 3 clearly shows that the main mechanisms were fiber thinning and breakage. These observations implied that CFs
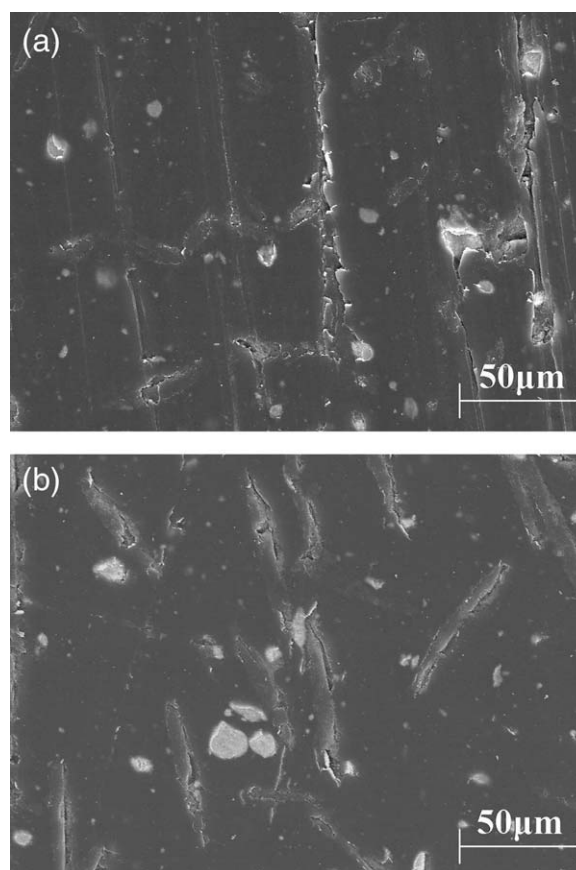
Figure 2 Effect of CFs on (a) the friction coefficient and (b) the wear rate of the PEEK/10ZrO$_2$ composites (test conditions: water lubrication, 2 m/s sliding velocity, and 2-h sliding duration).

slightly decreased as the fibers filled the composite. Within the studied range, the friction coefficient and wear rate of the PEEK composite filled only with ZrO$_2$ nanoparticles rapidly rose when the pressure was higher than 2 MPa. Both the friction coefficient and wear rate increased by 3 orders of magnitude as the load rose from 1 to 4 MPa. This implied that the tribological properties of the PEEK/10ZrO$_2$ composites severely deteriorated under high loads because of the lack of protection from the CFs. The friction test for the PEEK/10ZrO$_2$ composite could not be carried out at a load higher than 4 MPa because of severe vibrations of the test machine caused by the high frictional force, so no wear test data under 8 MPa are provided. However, the incorporation of 10wt% CF significantly improved the tribological performances of the composites: both the friction coefficient and the wear rate decreased dramatically. The friction coefficients of CF-filled PEEK/10ZrO$_2$ composites under loads higher than 2 MPa were still

Figure 3 Morphologies of the worn surfaces of the PEEK/10CF/10ZrO$_2$ composite under applied loads of (a) 1 and (b) 4 MPa (test conditions: water lubrication, 2 m/s sliding velocity, and 2-h sliding duration).
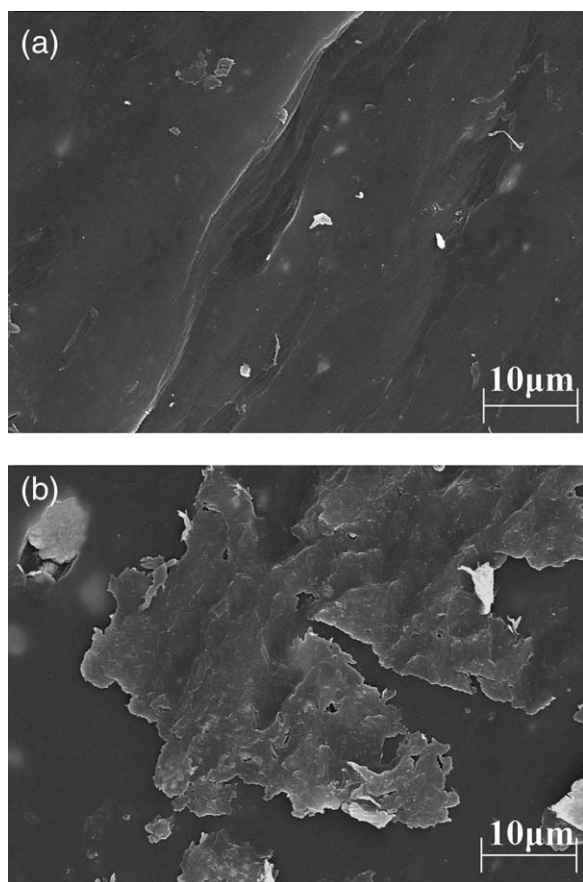
Figure 4 Typical morphologies showing (a) scuffing and (b) wear debris on the worn surfaces of the PEEK/10ZrO$_2$ composite under a load of 4 MPa (test conditions: water lubrication, 2 m/s sliding velocity, and 2-h sliding duration).

supported most stress during the sliding process. In this way, the matrix was protected from severe abrasion. This was also confirmed by the SEM morphologies of the PEEK/10ZrO$_2$ composite without CFs. As mentioned previously, the PEEK/10ZrO$_2$ composite showed bad performance at 4 MPa. Two typical morphologies of worn surfaces of the PEEK/10ZrO$_2$ composite at 4 MPa are illustrated in Figure 4(a,b). Obvious signs of scuffing and plastic deformation along with wear debris on the worn surface implied that the PEEK/10ZrO$_2$ composite suffered severe wear because of a lack of CFs. Without the main load-bearing phase in the surface layer, a large amount of wear debris was worn out when the load exceeded the critical value. This kind of wear debris might have acted as an abrasive third body on the sliding surfaces and might account for the severe vibrations of the test machine and badly deteriorated wear performance. The exfoliation on the worn surface indicated that there was fatigue–delamination behavior during the friction process.[30] Furthermore, the interfacial combination of the particles and the matrix was weakened in water with a high applied

load. The weak particle–matrix interface could act as crack nucleation and facilitate propagation of the fatigue crack on the subsurface. The cyclic stresses resulting from the contact of the composite surface with the hard asperity of the counterface led to fatigue wear and layer peeling on the pin surface. Accordingly, a large amount of sheet-form exfoliation accumulated on the worn surface and then fell onto the rubbing surface; this caused a severe abrasive effect on the composite. Actually, the friction force and the contact temperature were greatly increased when the pressure increased up to 4 MPa, and this further caused easier plastic flow and accelerative breakage of the matrix, especially in the interfacial region.

When there is sliding with a steel counterface under dry conditions, the formation of a transfer film is always thought to be an important factor enhancing the wear resistance of a polymer composite.[31] However, with water lubrication, the presence of water greatly inhibits the formation of the transfer layer by washing the wear debris away.[32,33] In this case, no obvious film formation was found on the hybrid composite's counterpart surface because the prepolished scratched marks still could be seen, as shown in Figure 5(a). Nevertheless, a thick and lumpy transfer film could be observed on the counterface for the PEEK/10ZrO$_2$ composite at 4 MPa [Fig. 5(b)]. Furthermore, lots of wear debris could be collected from the water. Figure 5(c) shows the wear debris gathered after the wear test of the PEEK/10ZrO$_2$ composite under 4 MPa. The debris was in the form of sheets, and this indicated fatigue–delamination behavior during the friction process.[30,34] Also, the presence of debris between the rubbing surfaces worsened the wear resistance of the composite and further roughened the counterface by forming a thick transfer film on it. Moreover, the high wear rate of 4.35×10^{-5} mm^3/Nm for the PEEK/10ZrO$_2$ composite under 4 MPa was also consistent with the large amount of transferred material. In other words, the presence of the transfer film and the wear debris was evidence of the severe wear in this case. In contrast, this kind of material transfer could not be detected for the PEEK/CF/ZrO$_2$ composites. The weight losses of the hybrid composites at loads ranging from 1 to 8 MPa were almost at the same level, that is, less than 0.3 mg (as shown in Table III). The height loss of the worn surface (Δh) could be roughly calculated with the following equation:

$$\Delta h = \frac{\Delta m}{\rho \cdot 3 \cdot \pi \left(\frac{d}{2}\right)^2} \tag{2}$$

where d is the diameter of the pin surface (mm). The densities of the hybrid composites ranged from 1.332 to 1.539 g/cm^3, and the diameter of the pin was 4.8
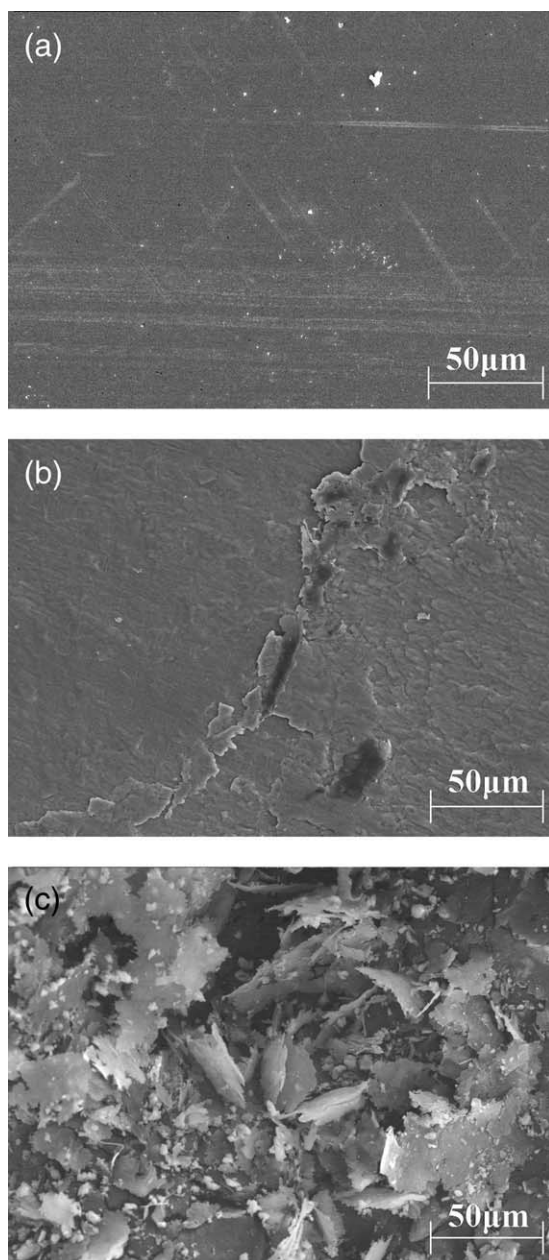
Figure 5 Morphologies of (a) the steel counterface of the PEEK/10CF/10ZrO$_2$ composite, (b) the steel counterface of the PEEK/10ZrO$_2$ composite, and (c) the wear debris of the PEEK/10ZrO$_2$ composite (test conditions: water lubrication, 2 m/s sliding velocity, 4-MPa applied load, and 2-h sliding duration).

mm. When the mass loss was assumed to be 0.3 mg, the height loss was determined to be 3.6–4.1 μm. This meant that the height losses of the composite pins at different loads were all less than 7 μm (i.e., the average diameter of the CFs). The wear of the composite pins was so low during the sliding process that the material losses at various loads were all less than one fiber layer. Therefore, the wear debris of the hybrid composites was hard to collect, and a transfer film could hardly be detected on the counterface. Furthermore, because the mass losses of the composites at different applied loads were all at the same level, the wear rates of the composites showed a decreasing trend as the pressure increased. Therefore, it is rational to say that CFs are the main reason for the outstanding antiwear properties of the PEEK/CF/ZrO$_2$ composites under aqueous conditions.

Effect of the ZrO$_2$ nanoparticles

Figure 6 shows the friction coefficient and wear rate of PEEK/10CF/ZrO$_2$ composites as functions of the ZrO$_2$ nanoparticle content. Figure 6(a) reveals that the friction coefficients of the PEEK/10CF composite were below the level of 0.01, and the applied loads had little influence on it. Under 1 MPa, when ZrO$_2$ nanoparticles at a concentration of 5 wt % were added to the PEEK/10CF composite, the friction coefficient of the composite increased rapidly, and this indicated that the nanoparticles slightly increased the friction coefficient of the composite under a low pressure. With the further addition of the nanoparticles to a concentration of 20 wt %, there was no obvious change in the friction coefficient. Under pressures higher than 2 MPa, however, the variation of the nano-ZrO$_2$ proportion had almost no effect on the friction coefficient of the composites.

As shown in Figure 6(b), the specific wear rates of the composites were obviously influenced by the nano-ZrO$_2$ content. The incorporation of 5 wt % nano-ZrO$_2$ led to a decrease in the specific wear rates of the PEEK/10CF composite. Then, the wear rates slightly rose with the nano-ZrO$_2$ content

TABLE III
Mass Losses of PEEK/CF/ZrO$_2$ Composites Under Different Loads

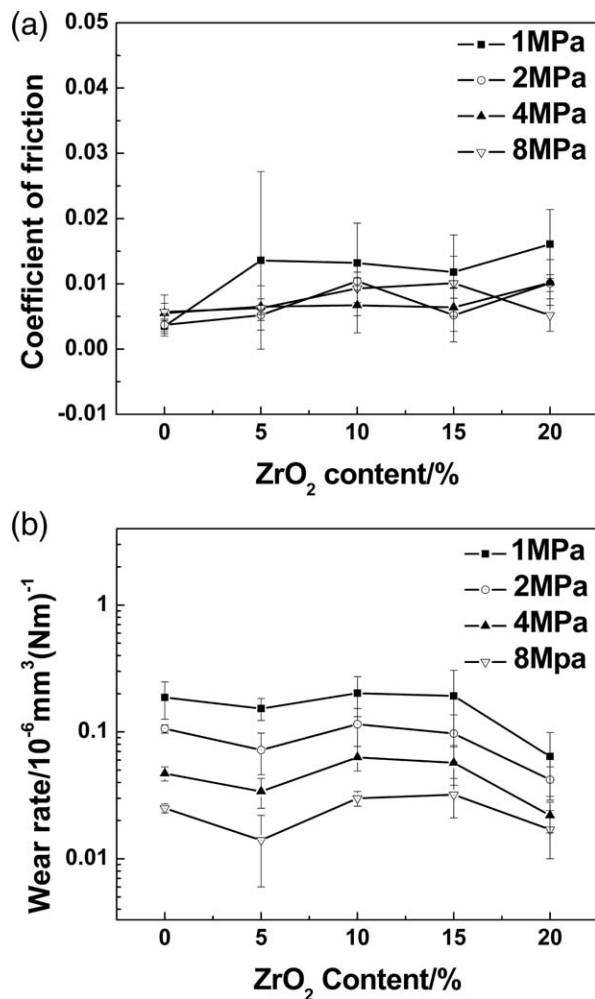| Load (MPa)	Mass loss (mg)						
	A1	A2	A3 (B2)	A4	A5	B3	B4
1	0.19 ± 0.06	0.16 ± 0.03	0.22 ± 0.07	0.22 ± 0.08	0.08 ± 0.05	0.23 ± 0.08	0.13 ± 0.07
2	0.22 ± 0.02	0.15 ± 0.05	0.25 ± 0.08	0.22 ± 0.05	0.1 ± 0.03	0.26 ± 0.07	0.19 ± 0.08
4	0.19 ± 0.02	0.14 ± 0.04	0.28 ± 0.06	0.26 ± 0.07	0.11 ± 0.03	0.28 ± 0.08	0.17 ± 0.05
8	0.21 ± 0.02	0.12 ± 0.06	0.27 ± 0.03	0.28 ± 0.08	0.16 ± 0.06	0.27 ± 0.07	0.16 ± 0.08

Figure 6 Effect of ZrO$_2$ nanoparticles on (a) the friction coefficient and (b) wear rate of the PEEK/10CF/ZrO$_2$ composites (test conditions: water lubrication, 2 m/s sliding velocity, and 2-h sliding duration).

increasing to 10 wt % and remained nearly unchanged until 15 wt % was achieved. With the further addition of nano-ZrO$_2$, the wear rate dropped remarkably and reached the lowest value. Similarly, increases in the pressure led to an evident decline of the wear rate, as shown in Figure 6(b).

To identify how ZrO$_2$ nanoparticles and CFs worked synergistically on the wear behavior of the hybrid composites, the worn surfaces of the PEEK/10CF and PEEK/10CF/5ZrO$_2$ composites are illustrated in Figure 7. Fiber thinning, debonding, and breakage could be found on both worn surfaces [Fig. 7(a,b)]. However, more microscuffing could be found on the worn surface of the ZrO$_2$-filled composite at 1 MPa. This might be attributed to the nanoparticles brushed from the matrix during the sliding process, which became abrasive at low pressures. Figure 7(c,d) shows that the worn surfaces with nanoparticles were much smoother, and the CF breakage, debonding, and peeling were greatly restricted with

the addition of 5% nano-ZrO$_2$ at 8 MPa. It is well known that the wear performance of SCF-reinforced polymer composites is governed mainly by fiber thinning, breaking, and peeling under dry-sliding conditions.[23,25] Fiber removal plays an important role in the wear mechanism. After the fiber peels off from the surface, the matrix is subjected to more intensive microploughing and microcutting attacks by steel asperities because of a lack of support and protection of the fibers, so more wear of the matrix can occur. With the incorporation of the nanoparticles, less fiber removal was observed on the worn surface for the hybrid composite, as shown in Figure 7(c,d). This should be attributed to the superior wear resistance of the PEEK/10CF/ZrO$_2$ composite under these conditions. To understand this advantage, we used high-magnification SEM images to observe typical fiber thinning and breakage on the worn surfaces of PEEK/10CF/5ZrO$_2$ and PEEK/10CF composites [Fig. 7(e,f)]. Obviously, although the main wear mechanisms were still fiber thinning and breakage for both composites, fiber debonding was greatly restrained by the incorporation of nanoparticles. In this way, the fibers could be maintained in the matrix. This led to an enhanced load-carrying capacity of the surface layer, which improved the wear resistance of the hybrid composites. For the PEEK/10CF composite, when the matrix material on and around the CFs was worn out, the CFs became exposed and suffered the impact of the asperities on the counterface. When the contact stress exceeded the load capacity, the CFs were cracked. However, the stress concentration on the CFs appeared to be reduced by the addition of the nanoparticles. This might be due to two factors. On the one hand, the reinforcement of the nanoparticles on the PEEK matrix could reduce the stress concentration at the fiber–matrix interface. On the other hand, a positive rolling effect of the nanoparticles between the material pairs took place during sliding, and this could reduce the shear stress between the two sliding surfaces. Moreover, the rolling effect also protected the SCFs from more severe wear mechanisms, especially at high sliding speeds and pressures.[23,25] In addition, the particles may have acted temporarily as distance holders between the rubbing surfaces and reduced the hard abrasion of the counterface to CFs.

Relationship between the mechanical properties and wear behavior

The effect of the filler content on the tribological behaviors of the hybrid composites might be explained by the variation of the mechanical properties to some extent. Actually, there have been many works studying the relationship between the mechanical properties and the tribological performances
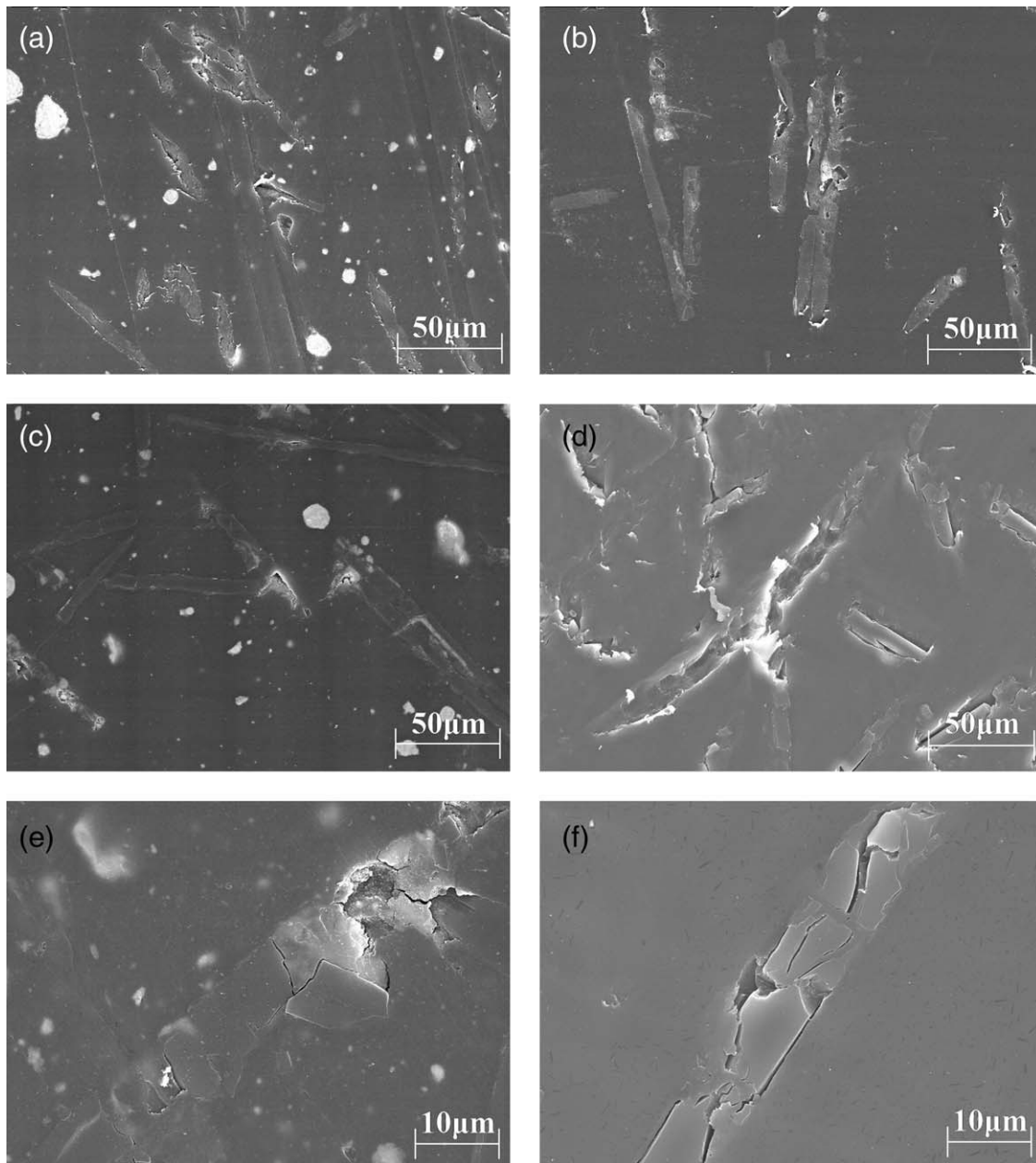
Figure 7 Morphologies of the worn surfaces of (a,c,e) the PEEK/10CF/ZrO$_2$ composite and (b,d,f) the PEEK/10CF composite.

of polymer–matrix composites.[35,36] Some mechanical properties of composites, such as the hardness, elongation at break, flexural modulus, and tensile strength, or a product of these factors usually has a significant influence on the wear behaviors of composites. Accordingly, materials possessing high stiffness and hardness can effectively resist deformation and crack propagation before fracture and, therefore, might achieve much lower specific wear rates. It is believed that the wear rate is a function of mechanical, tribological, and material parameters. A theoretical expression for the wear rate under lubricated conditions was derived from the concepts of crack propagation, damage accumulation, and classical mechanics by Lhymn.[37] According to this expression, the wear rate is inversely proportional to the product of the hardness (H), Young's modulus (E), and elongation at break (ε). In this case, as shown in Figure 8, the wear rates of PEEK/10CF/ZrO$_2$ composites with nanoparticle contents ranging from 5 to 20 wt % showed a high linear correlation to $1/HE\varepsilon$. The wear rate of the hybrid composites exhibited an increasing tendency with increases in the ZrO$_2$ content in the range of 5–15 wt % and further showed a strong drop-off trend when the ZrO$_2$ content reached 20 wt %.
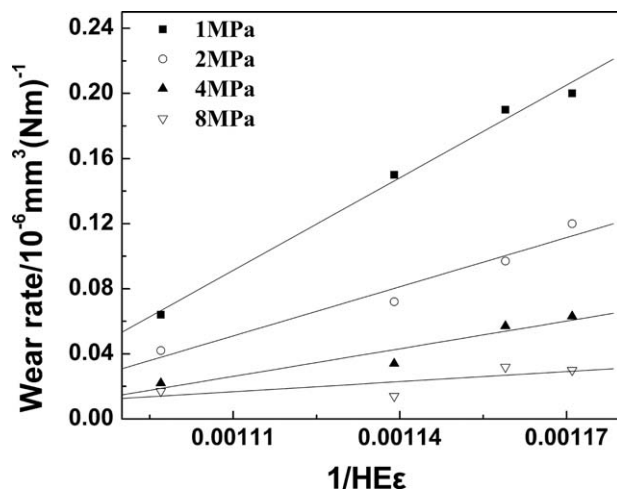
Figure 8 Wear rate of the PEEK/10CF/ZrO$_2$ composites (with the nano-ZrO$_2$ content varying from 5 to 20 wt %) versus 1/HEε.

As previously mentioned, the two fillers in the hybrid composites showed different influences on the mechanical performances. CF filling could significantly enhance the hardness and Young's modulus of the hybrid composites. However, the tensile strain at break sharply dropped as the fiber was compounded. Contrarily, the incorporation of the nanoparticles led to lower increases in the hardness and Young's modulus and also caused less deterioration of the elongation at break. Therefore, HEε could be regulated by changes in the proportions of the two fillers in the hybrid composites. In this way, we can expect optimized wear resistance to be achieved for the hybrid composites with the highest value of HEε. Further work should be devoted to obtaining more details about how the mechanical properties affect the wear behaviors.

CONCLUSIONS

The tribological properties of PEEK/CF/ZrO$_2$ composites under aqueous conditions have been investigated. The effects of CFs and nano-ZrO$_2$ on the wear behavior have been discussed. The following conclusions can be drawn:

1. The PEEK/CF/ZrO$_2$ composites possess excellent wear resistance under aqueous conditions because of a synergy effect between the ZrO$_2$ nanoparticles and CFs.
2. The CFs carry the main load between the contact surfaces and protect the matrix from further severe abrasion of the counterpart.
3. The incorporation of nano-ZrO$_2$ can efficiently inhibit CF failure in two ways: (1) by reducing the stress concentration on the CF interface through reinforcement of the matrix and (2) by

reducing the shear stress between two sliding surfaces via a positive rolling effect of the nanoparticles between the material pairs.
4. The wear rates of the hybrid composites are dependent on some mechanical properties. There is a good linear correlation between the wear rate and the product of the hardness, Young's modulus, and elongation at break.

References

1. Yamamoto, Y.; Takashima, T. Wear 2002, 253, 820.
2. Sumer, M.; Unal, H.; Mimaroglu, A. Wear 2008, 265, 1061.
3. Davim, J. P.; Marques, N.; Baptista, A. M. Wear 2001, 251, 1100.
4. Unal, H.; Mimaroglu, A. J Reinforced Plast Compos 2006, 25, 1659.
5. Voss, H.; Friedrich, K. Wear 1987, 116, 1.
6. Lu, Z. P.; Friedrich, K. Wear 1995, 181, 624.
7. Prehn, R.; Haupert, F.; Friedrich, K. Wear 2005, 259, 693.
8. Xu, L. J.; Davim, J. P.; Cardoso, R. J. Mater Process Technol 2007, 189, 374.
9. Yamamoto, Y.; Hashimoto, M. Wear 2004, 257, 181.
10. Jacobs, O.; Jaskulka, R.; Yan, C.; Wu, W. Tribol Lett 2005, 19, 319.
11. Wang, J. X.; Gu, M. Y. J Appl Polym Sci 2004, 93, 789.
12. Wang, O. H.; Xue, Q. J.; Shen, W. C. Tribol Int 1997, 30, 193.
13. Wang, Q. H.; Xu, J. F.; Shen, W. C.; Xue, Q. J. Wear 1997, 209, 316.
14. Wang, Q. H.; Xue, Q. J.; Shen, W. C.; Zhang, J. Y. J Appl Polym Sci 1998, 69, 135.
15. Xue, Q. J.; Wang, Q. H. Wear 1997, 213, 54.
16. Wang, Q. H.; Xu, J. F.; Shen, W. C.; Liu, W. M. Wear 1996, 196, 82.
17. Wang, Q. H.; Xue, Q. J.; Liu, H. W.; Shen, W. C.; Xu, J. F. Wear 1996, 198, 216.
18. Wang, Q. H.; Xue, Q. J.; Liu, W. M.; Chen, J. M. J Appl Polym Sci 2001, 79, 1394.
19. Wang, Q. H.; Xue, Q. J.; Liu, W. M.; Chen, J. M. J Appl Polym Sci 2000, 78, 609.
20. Zhang, M. Q.; Rong, M. Z.; Yu, S. L.; Wetzel, B.; Friedrich, K. Wear 2002, 253, 1086.
21. Zhang, M. Q.; Rong, M. Z.; Yu, S. L.; Wetzel, B.; Friedrich, K. Macromol Mater Eng 2002, 287, 111.
22. Chang, L.; Zhang, Z.; Breidt, C.; Friedrich, K. Wear 2005, 258, 141.
23. Chang, L.; Zhang, Z. Wear 2006, 260, 869.
24. Zhang, G.; Chang, L.; Schlarb, A. K. Compos Sci Technol 2009, 69, 1029.
25. Jiang, Z. Y.; Gyurova, L. A.; Schlarb, A. K.; Friedrich, K.; Zhang, Z. Compos Sci Technol 2008, 68, 734.
26. Chang, L.; Zhang, Z.; Ye, L.; Friedrich, K. Tribol Int 2007, 40, 1170.
27. Meng, H.; Sui, G. X.; Fang, P. F.; Yang, R. Polymer 2008, 49, 610.
28. Borruto, A.; Crivellone, G.; Marani, F. Wear 1998, 222, 57.
29. Jia, J.; Chen, J.; Zhou, H.; Hu, L. Tribol Lett 2004, 17, 231.
30. Zhang, M. Q.; Lu, Z. P.; Friedrich, K. Tribol Int 1997, 30, 103.
31. Bahadur, S. Wear 2000, 245, 92.
32. Srinath, G.; Gnanamoorthy, R. Compos Sci Technol 2007, 67, 399.
33. Lancaster, J. K. Wear 1972, 20, 315.
34. Ovaert, T. C.; Cheng, H. S. Wear 1991, 150, 275.
35. Bijwe, J.; Sen, S.; Ghosh, A. Wear 2005, 258, 1536.
36. Rajesh, J. J.; Bijwe, J.; Tewari, U. S. J Mater Sci 2001, 36, 351.
37. Lhymn, C. Wear 1988, 122, 13.